

DESIGN OF A WIND TUNNEL SCALE MODEL OF AN ADAPTIVE WIND TURBINE BLADE FOR ACTIVE AERODYNAMIC LOAD CONTROL EXPERIMENTS

Anton W. Hulskamp*, **Adriaan Beukers*****, **Harald E.N. Bersee***,
Jan Willem van Wingerden *** and **Thanasis Barlas******.

***Design and Production of Composite Structures, Faculty of Aerospace Engineering,
Delft University of Technology, Kluyverweg 1, 2629 HS Delft, The Netherlands**

****Fellow Professor Doshisha University, Kyoto, Japan**

*****Delft Center for Systems and Control, Delft University of Technology, The Netherlands**

******Wind Energy Department, Faculty of Aerospace Engineering,
Delft University of Technology, The Netherlands**

Abstract

Within wind energy research there is a drive towards the development of a “smart rotor”; a rotor of which the loading can be measured and controlled through the application of a sensor system, a control system and an aerodynamic device. Most promising solutions from an aerodynamic point of view are trailing edge flaps, either hinged or continuously deformable. An experiment was considered necessary in which the effectiveness of such a system, with the interaction between dynamics, aerodynamics and control was tested. In order to perform this experiment, a blade needed to be constructed that had the scaled dynamics of a full scale blade as well as sufficient actuation power and sensors for measurements as well as feedback control. A blade was designed and tested with sufficient strength for high wind speed as well as an eigenfrequency (12.5Hz) that was close to the initial value (19.2Hz), derived from scaling the dynamics. Finally adapting the airspeed set the right dynamics. System identification was performed and a controller designed with which a significant reduction in vibrations was attained.

1 Introduction

Wind turbine blades are constantly subjected to fluctuating loads. On top of the mean aerodynamic load there are several disturbances that cause

variations in the bending moment at the root of the blade. These variations are caused by changes in the wind field and by the rotation of the blade through this wind field. Examples of these are wind shear, tower shadow and turbulence.

Moreover, there is a trend in wind turbine engineering to produce turbines of ever increasing size, mainly for off-shore purposes. The current limit is a 120m rotor diameter and ever larger dimensions are expected in the near future. See figure 1.

The increase in size is driven by the fact that the power conversion of a wind turbine increases with the square of the rotor blade’s diameter. However, this causes mass effects to play a larger role in the design of turbines. Additionally, because the rotor rotates with respect to the gravitational field, these gravity effects also cause fluctuations in the root bending moment.

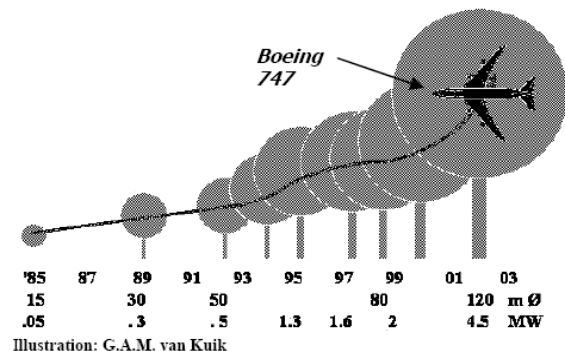


Fig. 1. Increase in wind turbine size over the past decades.

All these effects cause serious fatigue problems for turbine blades and fatigue is therefore also the main design drive for most wind classes. Current blades are dimensioned for at least 10^8 cycles [1]. Structurally, the main concern in this is bending in flap wise direction since lift forces are the highest forces on the blade but the blade has the lowest resistance to bending in that direction.

However, instead of dimensioning the blade for these fatigue loads which is done today, mitigating these loads through controlling the aerodynamics of the blade is also an option. Such an aerodynamic load control (ALC) system has been intensively researched for helicopter blades [2], [3], and recently also some feasibility studies for wind turbine blades have been made [4], [5]. The goals of such a system would be to react both to deterministic loads, such as wind shear and tower shadow, as to undeterministic loads such as gusts.

Nevertheless, most studies into ALC are mainly aimed at showing the potential of the aerodynamic part or they present actuator concepts for helicopter rotors. The interaction with the dynamics of the structure and the issues concerning control are sparsely researched. Therefore it was decided to conduct an experiment where the dynamics of the blade are of importance for the occurring disturbances, as well as the aerodynamics and control issues.

2 General set-up

2.1 Wind tunnel set-up

A full scale wind turbine blade is tapered and has twist to accommodate for the change in experienced wind speed and angle. However, it was chosen as a first approach to perform these experiments on a non-rotating blade, not taking into account the twist, taper and thickness distribution of the blade. This meant that the blade can be regarded as a clamped beam with uniform cross-section. The blade is attached to a pitch system at the wind tunnel wall and free to deflect over a table at the free end. The pitch system can be used to change the mean angle of attack, as well as inducing the aerodynamic disturbances that are to be researched. The table would ensure that there are no tip-effects, because only 2D aerodynamic analyses were made. This way, quasi 2D flow would be obtained in the static case. See figure 2 for a sketch of the set-up. However, additionally experiments without table were also performed.

For controlling the aerodynamic loads it was chosen to implement partial camber control: the aft half of the cord at certain stations in the outboard section of the blade was made deformable therefore allowing for a change in camber of that piece of the cord. Such ALC systems were also suggested for wind turbine blades by Buhl [4] and Joncas [5]. The actuator is based on a piezo electric bender.

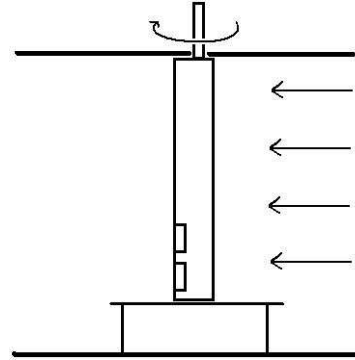


Fig. 2. Sketch of the wind tunnel set-up: non rotating, pitchable blade, clamped at one side. Tip effects are suppressed by the presence of the table.

2.2 Control

In order to control the actuators and read the signals from the sensors, a dSpace™ system was employed for both feed forward as feedback experiments. With this systems sensors signals are converted to a digital signal and sampled. These signals can be recorded as well as fed to a feedback control algorithm. The output of the control system (whether it's feedforward or feedback) is converted to an analogue signal and send to the different actuators. The system of processing signals as well as the feedback controller is designed in Simulink™ and compiled onto the dSpace™ system. In- and outputs for e.g. setting values and plotting and recording signals can also be incorporated and linked to Control Desk™, a Graphical User Interface (GUI). See figure 3.

From the dSpace™ hardware, one signal goes to the pitch system, which consists of a linear motor and two signals go to the high voltage amplifier which drives both sets of piezo electric benders.

Inputs to dSpace™ include: the actual pitch displacement (feedback from the pitch system), the actual voltage on the piezo electric benders (output of the amplifier), strain at the root of the blade and acceleration of the tip.

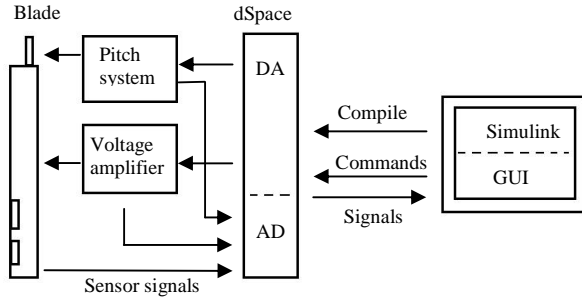


Fig 3. Set-up of the control system.

3 Blade dynamics

As mentioned, the importance of this experiment was to tune the dynamics to the aerodynamics to obtain a representative scale model to control. The most important scaling parameter, is the reduced frequency. The reduced frequency k is defined as

$$k = \omega b / V \quad (1)$$

In which k is called the reduced frequency, ω the frequency of the disturbances, V the undisturbed airspeed and b the half cord of the aerofoil. With it, frequencies of disturbances can be scaled to the dimensions of the blade and the wind speed. The aerodynamic delay, the phase between a sine on the flap and the resulting lift forces, is dependent on this reduced frequency [6].

The wind tunnel blade has a 120mm cord and it was chosen to perform the experiment at 70m/s because of the range of the wind tunnel and the expected loads. A reference turbine blade that was used to scale our model to, has a first flapping eigenfrequency of 1Hz. The relevant geometrical and air speed data were taken from the $R=0.75$ station, which would be the location for the flaps on a full scale turbine. Moreover, the rotational frequency and thus the frequency of the 1P loads – e.g. wind shear, gravity effects- for this turbine is 0.28Hz. That puts the 3P loads at 0.84Hz, close to the eigenfrequency. All these frequencies had to be tuned to our model's size and the air speed of the wind tunnel to attain the appropriate reduced frequencies. In table 1 an overview of the parameters is presented.

Table 1. Scaling parameters for the wind tunnel model

	Reference blade	Wind tunnel model (goal)
Air speed	54m/s	70m/s
Cord	1.8m	0.12m
Eigenfrequency	1Hz	19.2Hz
Frequency of 1P loads	0.28Hz	5.5Hz
Frequency of 3P loads	0.84Hz	16.6Hz

4 Blade design

4.1 Sensors

For control purposes, the blade was equipped with sensors which recorded its dynamic behaviour. Because the final goal was to minimize the variations in blade root moment, a PZT patch was adhered at the root where the thickness of the airfoil is maximal, thus recording the strains there. This sensor's signal was also used to serve as feedback for the controller. An accelerometer was also fitted inside the tip. Unfortunately, a usable signal was only observed at high frequencies due to its limited size.

4.2 Actuator

As explained, the blade was equipped with actuators in outboard part of the blade. The active part of the actuators consisted of Thunder[®] TH-6R actuators. These are piezo electric based benders deflect several millimetres under the application of a maximum AC voltage of 900V, peak-peak. The actual deflection also depends on the structure around it and the aerodynamic loading. Unfortunately, the deflection shows a non-linear behaviour with the voltage. This is because due to an intentional mismatch in coefficient of thermal expansion of the different layers and production at elevated temperature, the actuator is domed, which reduces its intrinsic stiffness and allows it to deflect further than would be predicted by linear beam theory [7]. The actuators were shaped with soft foam to give them their aerodynamic shape. The foam was covered with a latex skin to provide a smooth surface. A perfect aerofoil shape was not attained, but the goal is to change the aerodynamics, not to maximize aerodynamic performance. The actuators were attached to the blade through a bracket that was mounted on the spar. See figure 4 for the outline of the flaps.

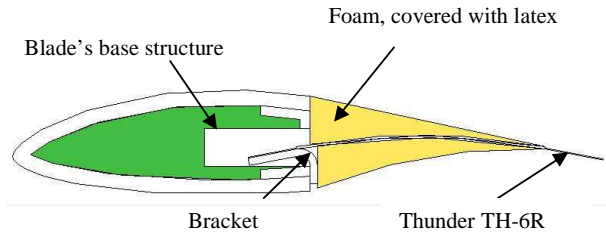


Fig. 4. Design and mounting of the actuator

4.3 Structural design

The outer shape of the blade was given by the shape of the DU96-W-180 aerofoil with 0.12m cord. However, the internal structural design could be filled in freely within these geometrical constraints. The design requirements for stiffness and strength were determined. Safety factors were chosen to account for higher loads due to for instance a failure in control, dynamic stall and vibration of the blade. $C_L=3$ and an $V=100\text{m/s}$ was calculated with.

As mentioned before, the blade had to have an eigenfrequency of 19.2Hz. There is some room for deviations in this, because the other factor which determines the reduced frequency is the air speed in the wind tunnel which can also be chosen. However, with this the margin for error is limited: a too high air speed would result unallowable loads, a too low airspeed would result in a too low sensor signal and low actuator effectiveness.

The blade was constructed in three different sections. This is because the tip sections, in which the actuators were mounted, is also to be used in a future, rotating experiment. The blade in that experiment will require a root with twist, taper and a thickness distribution. The blade for the non-rotating case, which is discussed here, has a uniform cross-section. It was therefore decided to use the mould for the tip also to produce two more sections which form the root sections. The three sections were bolted together after production.

The global design is very basic and was mainly driven by the production process. The blade's section were produced by vacuum infusing a dry preform which consisted of a number of glass fibre 8H-satin plies folded around a foam core. This preform was placed in the cavity of a rigid mould, assuring an aerodynamic viable surface on both sides. Finally, the resin was infused. At each end of the foam an anodized aluminium insert and if required, a prefabricated spar could be placed in the

foam core. Special precautions were taken in positioning the inserts in the mould since that ensured a good fit of the sections on each other. The spar was given a 'U'-shape to ensure adhesion to the skin. See figure 5. Only 0° plies were considered for both the spar and skin due to production considerations.

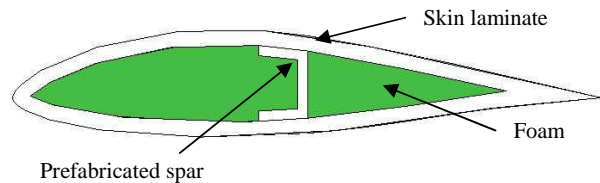


Fig. 5. Internal lay-out of the blade

The finite element analysis was performed in Abaqus. The model was set up as follows: Skin and spar were modelled using four node shell elements. The position of the shell's plane in the laminate was shifted to the outer ply – the default is the centre ply – so the geometry described by the elements agreed with the actual outer contour of the laminate and thus of the aerofoil. The foam and aluminium inserts were modelled using eight node brick elements, or wedges where needed. The shell elements can be observed in figure 6.

To determine the material properties from the constituents, the fibre volume fraction has to be determined. In the design on the foam and the mould

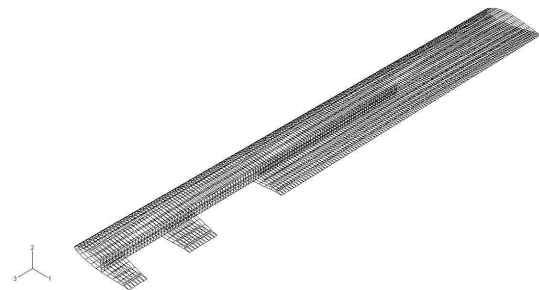


Fig. 6. Shell elements of the blade's FE model

0.25mm thickness per glass ply was taken into account. Since the dimensions of the laminate were fixed by the rigid mould and foam and it was known how many glass would be placed in the mould, the fibre volume fraction could be derived. Subsequently, a micromechanical model was employed to determine the material properties. The spar was prefabricated with vacuum infusion under flexible tooling, which resulted in a higher fibre

volume fraction. This was determined by burning of the matrix. The fibre volume fractions and used material parameters are displayed in table 2.

Table 2. Material properties

	Skin	Spar
V_f	0.484	0.508
E_{11} [GPa]	21.33	22.94
E_{22} [GPa]	20.86	22.47
E_{33} [GPa]	9.07	9.53
ν_{12}	0.138	0.143
ν_{13}	0.258	0.256
ν_{23}	0.258	0.257
G_{12} [GPa]	4.51	5.17
G_{13} [GPa]	4.55	5.2
G_{23} [GPa]	4.54	5.2

Strength parameters were estimated and the Tsai Hill criterion was used for estimating the strength. The design was evaluated for staying within the limits of the criterion.

Boundary conditions and loading consists of clamping at the root and a lift force distributed over the blade. This was implemented by restricting all translational degrees of freedom at the root and applying a uniform pressure distribution which equals the lift force over the whole surface of the blade. Half of this was applied to the suction and the other half to the pressure side. The connection between the sections was modelled by using contact elements and the bolts by beam elements which were pretensioned by assigning them with a coefficient of thermal expansion and applying a temperature difference.

The process of detailing the design was iteratively performed in Abaqus. The following parameters were considered and the results are displayed in table 3:

- Number of plies in the skin
- Number of plies in the spar (or absent spar)

Table 3. Laminate build-up for spar and skin

	Blade root (section 1)	Outboard sections (2&3)
Skin	20 plies, t=5mm	12 plies, t=3mm
Spar	-	9 plies, t=2mm

The eigenfrequency was predicted to be 15.8Hz and the maximum Tsai Hill criterion number was 0.82, reached at the root in the skin laminate.

The spar was omitted from the root section for various reasons:

- it was determined that the laminate would become so thick that adding a spar in was of little added value
- The stresses in the spar would become quite large, because only 0° plies were applied and the spar is loaded in shear.
- It would require another spar mould and production step, while the analysis pointed out that application of the spar was not necessary.

4.4 Verification

Two types of experiments were conducted to verify the mechanical properties. First of all a static experiment: Two three point bending tests were performed on the two types of sections; one without the spar and with the thick laminate and one on the one with the thinner laminate and with spar. Each segment was loaded and unloaded four times and the data was very consistent.

The same type of load case was also analyzed with the FE model and the results compared. The results are displayed in table 4. The values correspond well.

Table 4. Bending stiffness, derived from three point bending test in experiments and FEM

	Outboard section	Inboard section
EI three-point-bend test [Nm^2]	456	530
EI FE model [Nm^2]	482	492
Deviation from experiments	+5.7%	-7.1%

Secondly, the dynamic properties of the system were determined during system identification. The eigenfrequency was found to be 12.5Hz, where 15.8Hz was predicted. This a part of this can be attributed to discretizing with FEM, but also in the dynamic analysis the mass of the cables and lightweight actuators was not accounted for. Due to the lower eigenfrequency, the wind speed had to be lowered further to 45m/s to still end up at the appropriate reduced frequency. This is still well within limits to measure a signal and to attain sufficient aerodynamic efficiency from the flaps.

5 Preliminary experimental results and blade performance

The blade will be employed in several experiments. The results of the first set are promising. In these experiments a step, simulating a gust, was put on the pitch of the blade which triggered a sudden change in lift. This was firstly done without controlling the flaps and secondly with feedback control. The results in three cases, $\alpha=0$, $\alpha=6$ (around maximum C_L/C_D) and $\alpha=10$, can be seen in figures 7, 8 and 9. A significant reduction in the vibration behaviour, as well as a reduction of the overshoot in the first peak can be observed.

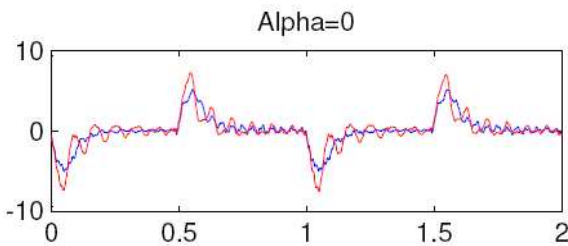


Fig. 7. Strain signal at the root as a result of a step on the pitch at zero angle of attack

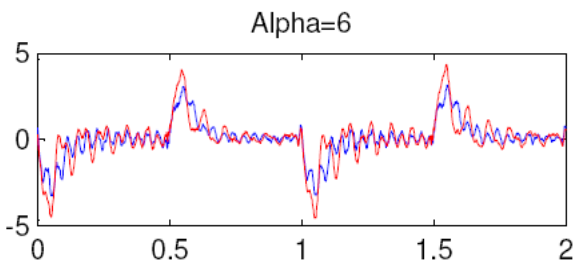


Fig. 8. Strain signal at the root as a result of a step on the pitch at 6° angle of attack (close to maximum C_L/C_D , desired operating point for the DU-96 aerofoil)

In addition, the blade was excited with a sine on the pitch and the flaps were controlled to compensate for the change in lift. The effects of aerodynamic delay were not observed in these experiments because the delay due to the pitching is the same as that of the counteracting flap motion.

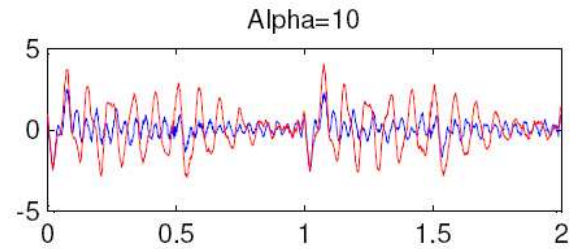


Fig. 9. Strain signal at the root as a result of a step on the pitch at 10° angle of attack (higher than the static stall angle).

Future experiments will include testing other aerodynamic devices, such as microtabs [8] or upscalable trailing edge flaps, as well as analyzing the unsteady flow around the blade.

6 Conclusions

Blade performs as planned. The deviations from the predicted eigenfrequency could easily be compensated by a change in air speed in the wind tunnel. This was done twice: once because the predicted behaviour did not match the wanted behaviour and secondly because the actual behaviour did not match the predicted behaviour.

The dynamics of the blade are important because any disturbance will cause the blade to resonate in its first eigenmode. This effect is amplified because the first eigenfrequency is close to that of the 3P loads. To perform sensible experiments, these dynamics should match those of the full scale blade.

The main issue is with the sensors. There is little room for accelerometers. Moreover the actual performance of the flaps was hard to study since there was no internal feedback loop on the Thunder[®] actuators. The control system performs well, nevertheless, and a significant reduction in the fatigue spectrum was observed. Future experiments in aerodynamics and other actuator types should provide more answers.

Acknowledgements

This research was conducted within the framework of the UpWind project of the European Union. The research is supported by the Technology Foundation STW, applied science division of NWO and the technology program of the Ministry of Economic Affairs. The project was initiated and coordinated

through the DUWind institute at the Delft University of Technology.

References

- [1] Nijssen R.P.L. “*Fatigue Life Prediction and Strength Degradation of Wind Turbine Rotor Blade Composites*”, PhD dissertation, Faculty of Aerospace Engineering, Delft University of Technology, The Netherlands, 2006.
- [2] Koratkar N.A. and Chopra I., “Wind tunnel testing of a Mach-scaled rotor model with trailing-edge flaps”, *Smart Materials and Structures*, Vol. 10, pp1–14, 2001.
- [3] Straub F.K., Ngo H.T., Anand V. and Domzalski D.B., “Development of a piezoelectric actuator for trailing edge flap control of full scale rotor blades”, *Smart Materials and Structures*, Vol. 10, pp 25–34, 2001.
- [4] Buhl T., Gaunaa M., Bak C., “Load Reduction Potential Using Airfoils With Variable Trailing Edge Geometry”. *43rd AIAA Aerospace Sciences Meeting and Exhibit*, Reno, Nevada, Jan. 10-13, pp 1-18, 2005
- [5] Joncas S., Bergsma O. and Beukers A., “Power Regulation and Optimization of Offshore Wind Turbines through Trailing Edge Flap Control”, *Proceedings of the 43th AIAA Aerospace Science Meeting and Exhibit*, 10-13 January 2005, Reno, Nevada.
- [6] Leishman J.G., “Unsteady Lift of a Flapped Airfoil by Indicial Concepts”. *Journal of Aircraft*, Vol. 31, No. 2, pp 288-297, 1994.
- [7] Aimmanee S. and Hyer M.W., “Analysis of the manufactured shape of rectangular THUNDER-type actuators”, *Smart Materials and Structures*, Vol. 13 pp 1389–1406, 2004.
- [8] Yen Nakafuji D.T., van Dam C.P., Michel J.,Morrison P., “Load Control for Turbine Blades: a Non-traditional Microtab Approach”. *2002 ASME Wind Energy Symposium; AIAA Aerospace Sciences Meeting and Exhibit, 40th, Collection of Technical Papers*, Reno, Nevada, Jan. 14-17, pp 321-330, 2002.